2010 IEEE International Conference on Robotics and Automation
Anchorage Convention District
May 3-8, 2010, Anchorage, Alaska, USA

Control of a High Fidelity Ungrounded Torque Feedback Device: The iTorqU 2.1

Kyle N. Winfree*, Joseph M. Romano†, Jamie Gewirtz†, and Katherine J. Kuchenbecker†

*Mechanical Systems Laboratory
University of Delaware, USA
winfree@udel.edu

†GRASP Laboratory, MEAM Department
University of Pennsylvania, USA
{jrom,gewirtzj,kuchenbe}@seas.upenn.edu

***Abstract*— This paper outlines how a control moment gyroscope can be used to generate haptic torque feedback while minimizing the effects of a constrained gimbal workspace. We present the design of the iTorqU 2.1 and discuss how it compares to previously developed systems. We then detail the control algorithms we have developed for both transparency and torque output modes. The prescribed transparency controller is typical in design, but the torque output algorithm is novel to this type of haptic device. It makes use of a series of position-p-at-time-t commands, which we call packets. Five packet designs were considered in this research, but we have included only the most important three in this paper. While this research deals with torque feedback, it ultimately presents a method for working with devices that are limited by the need for continuous reset to a home position before subsequent outputs.**

I. Introduction

Reorienting a spinning flywheel causes a torque about the axis that is perpendicular to both the flywheel axis and the axis of the imposed rotation [3]. An analysis of gyroscope dynamics reveals that the magnitude of the torque created by such a motion generally exceeds the torque delivered by reorienting the same flywheel when it is not spinning. As shown in Figure 1, we have used this principle to create a custom haptic device that delivers ungrounded torque feedback to the hand of a user. The iTorqU 2.1 is composed of a flywheel mounted in a two-degree-of-freedom motorized gimbal which is attached to a handle. We believe that devices like this could be useful in applications such as rehabilitation and computer gaming, where users want to feel haptic feedback when they interact with items in a virtual environment. The gyroscopic effect offers a means for creating ungrounded haptic devices that can apply significant torques to the hand of a user throughout a workspace that is much larger than what is possible with traditional desktop haptic interfaces.

We presented the preliminary design for the iTorqU 2.0 in a previous conference paper [7]. After reviewing related haptic devices, this paper describes the design changes that were made for version 2.1. We then present our dynamic model of this device, and we explain the controllers we developed to facilitate its use as a haptic interface. Understanding the dynamics and control of the iTorqU has been essential for the development of this system, and we hope it may be useful to others developing similar systems.

Fig. 1: The iTorqU 2.1.

II. Previous Research

Though there have been other ungrounded torque feedback devices [4] [5], the one most similar to the iTorqU is the Gyro Moment Display [8] by Yano et al. Like the iTorqU, the Gyro Moment Display makes use of the gyroscopic effect by mounting a cylindrical mass in a Cardan suspension gimbal; it can thus generate torques orthogonal to both the rotational axis of the flywheel and the actuated gimbal axis. The rotational inertia of the flywheel was designed to be sufficiently large such that when the flywheel spins very quickly, small perturbations in the gimbal configuration result in significant output torques. In their discussion of this system, Yano et al. noted success at generating ungrounded arbitrary output torques, but they acknowledged that the limited workspace of the gimbal imposed a delay while the flywheel returned to its home position in preparation for another arbitrary torque. Subsequent work on the Gyro Moment Display [9] included an alternative method that took into consideration the orientation and motion of the user's arm to generate torques about an arbitrary axis. The authors used this method to compensate for the motion of their device. A key difference between our work and [9] is that this prior approach did not consider the effect of rotating gimbal axes during torque output events, which we observe and attempt minimize.

978-1-4244-5040-4/10/$26.00 ©2010 IEEE

III. Changes from the iTorqU 2.0

Our first prototype of the second generation iTorqU was called the iTorqU 2.0 [7]. This device had two actuated axes on the gimbal and a drum-capstan gimbal transmission. Upon testing version 2.0, we found that the motors used were not strong enough to generate our desired output torques given the device's drum-capstan gear ratio. In version 2.1, shown in Figure 1, these motors were replaced with Maxon 118730 4.5 watt RE 16 motors each fitted with a Maxon 110321 planetary gear head with a gear ratio of 4.4:1. This change proved sufficient for generation of the desired torques without significantly influencing the backdrivability of each gimbal axis. A Maxon 110778 encoder with a quadrature resolution of 64 counts per turn also replaced the previous hall-effect sensors. To accommodate these longer motors, the motor-gimbal arrangement was changed, with the top motor now placed inside the upper gimbal. This alteration also helps to minimize the inertia effects of the motor. In addition, the drum on this upper gimbal was redesigned to provide the needed clearance for the flywheel. This change resulted in a drum-capstan gear ratio of 14.5:1, 1.44 times larger than the original drum-capstan gear ratio of 10.1:1. The new motor could be accommodated without changes to the bottom drum; the original gear ratio remains. Finally, the inertial measurement unit was reoriented to make the best use of the internal compass and accelerometers.

IV. Controller Design

The ideal haptic device has two very important characteristics [2] [1]. First, it is transparent. This means that the user cannot feel its presence when no outputs are desired. Second, the ideal haptic device is able to produce the desired sensations when requested. In order to achieve both of these goals, the iTorqU has two active control modes: a transparency controller and an active torque output controller. Our torque output controller uses *position-p-at-time-t* commands that allow for the creation of the desired outputs while also minimizing undesired outputs. To support the presentation of these high-level controllers, we first discuss dynamic modeling and low-level control.

A. Dynamic Model

The total output torque of the iTorqU device can be described by a sum of all contributing torques. This includes the torques due to the reorientation of the flywheel, the movement of the top and bottom gimbals, and the weight of each gimbal. This sum can be written as

$$\begin{aligned} {}^h\vec{M}_{total} = {}& {}^h\vec{M}_{(I\ fw)} + {}^h\vec{M}_{(I\ top)} + {}^h\vec{M}_{(I\ bottom)} + \\ & {}^h\vec{M}_{(gravity\ top)} + {}^h\vec{M}_{(gravity\ bottom)} \end{aligned} \tag{1}$$

where ${}^h\vec{M}_{total}$ is the total torque in the handle frame, ${}^h\vec{M}_{(I\ fw)}$ is the torque contributed by the flywheel's inertia, ${}^h\vec{M}_{(I\ top)}$ and ${}^h\vec{M}_{(I\ bottom)}$ are the torques contributed by the top and bottom gimbals respectively, and ${}^h\vec{M}_{(gravity\ top)}$ and ${}^h\vec{M}_{(gravity\ bottom)}$ are the torques contributed by gravity acting on the top and bottom gimbals.

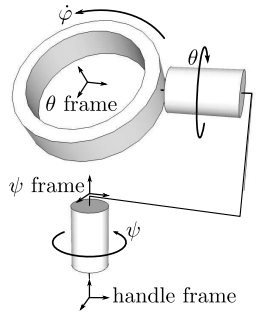

Fig. 2: The Cardan suspension gimbal and its reference frames.

We will consider only the torques contributed by the flywheel in this section, though the model used in later sections does include all five components of (1). The device's reference frames are shown in Figure 2. In the frame of the last gimbal, θ, the flywheel's output torque is:

$${}^\theta\vec{M}_{fw} = \mathbf{I}\cdot\dot{\vec{\omega}}_{system} + \vec{\omega}_{frame}\times(\mathbf{I}\cdot\vec{\omega}) \tag{2}$$

In matrix form the detailed equation can be expressed as:

$$\begin{aligned} {}^\theta\vec{M}_{fw} = {}& \begin{bmatrix} I_{xx} & 0 & 0 \\ 0 & I_{xx} & 0 \\ 0 & 0 & I_{zz} \end{bmatrix} \cdot \begin{bmatrix} -\ddot{\psi}\sin\theta - \dot{\psi}\dot{\theta}\cos\theta \\ \ddot{\theta} \\ \ddot{\varphi} + \ddot{\psi}cos\theta - \dot{\psi}\dot{\theta}\cos\theta \end{bmatrix} \\ & + \begin{bmatrix} -\dot{\psi}\sin\theta \\ 0 \\ \dot{\psi}\cos\theta \end{bmatrix} \times \begin{bmatrix} I_{xx} & 0 & 0 \\ 0 & I_{xx} & 0 \\ 0 & 0 & I_{zz} \end{bmatrix} \cdot \begin{bmatrix} \dot{\psi}\sin\theta \\ 0 \\ \dot{\varphi} + \dot{\psi}\cos\theta \end{bmatrix} \end{aligned} \tag{3}$$

where $I_{yy} = I_{xx}$ because of the flywheel's symmetry. Now, if we apply the appropriate coordinate frame rotation to this torque, the output torque generated by the flywheel in the handle frame is:

$$\begin{aligned} {}^h\vec{M}_{fw} = {}& {}^h\mathbf{R}_\theta \cdot {}^\theta\vec{M}_{fw} \\ = {}& \begin{bmatrix} \cos\psi\cos\theta & \sin\psi & -\cos\psi\sin\theta \\ -\sin\psi\cos\theta & \cos\psi & \sin\psi\sin\theta \\ \sin\theta & 0 & \cos\theta \end{bmatrix} \cdot {}^\theta\vec{M}_{fw} \end{aligned} \tag{4}$$

This shows that the orientation, angular velocity, and angular acceleration of the flywheel and gimbal are all very important in determining the output torque. Consequently, a robust low-level controller is important to ensure that the desired gimbal configuration is achieved.

B. Low Level Control

Both iTorqU control modes use a low level position controller that operates at approximately 1000 Hz. The output torque of the motor that drives each gimbal axis is determined by the following:

$$\begin{aligned} \tau_\psi &= k_\psi(\psi_{des} - \psi_{act}) - k_{\dot{\psi}}(\dot{\psi}_{des} - \dot{\psi}_{act}) \\ \tau_\theta &= k_\theta(\theta_{des} - \theta_{act}) - k_{\dot{\theta}}(\dot{\theta}_{des} - \dot{\theta}_{act}) \end{aligned} \tag{5}$$

where τ is the motor's output torque, k_ψ and k_θ are position gains ($(N\cdot m)/^\circ$), and $k_{\dot{\psi}}$ and $k_{\dot{\theta}}$ are velocity damping gains ($(N\cdot m)/(^\circ/s)$). ψ_{des} and ψ_{act} are the desired and actual ψ angles respectively. The same convention holds for θ_{des}, θ_{act}, $\dot{\psi}_{des}$, $\dot{\psi}_{act}$, $\dot{\theta}_{des}$, and $\dot{\theta}_{act}$.

C. Transparency

To enable transparency, the instantaneous orientation of the handle is estimated by an inertial measurement unit (Microstrain model GX1). The controller uses these estimated angles as the desired gimbal angles to keep the gimbal in a stationary configuration relative to the ground frame. Data from the inertial measurement unit is sampled at approximately 70 Hz. To account for the low refresh rate of the inertial measurement unit, our software differentiates the gimbal angles at 1000 Hz. For example,

$$\dot{\psi}_{i\ raw} = \frac{\psi_i - \psi_{i-1}}{t_i - t_{i-1}} \tag{6}$$

A low-pass filter with a cutoff frequency of 1.6 Hz is used to smooth our velocity calculations to create a better estimate of both $\dot{\theta}_{raw}$ and $\dot{\psi}_{raw}$ for the position controller in (5). In the transparency mode, the control gains for (5) are set to k_θ = 0.75 $(N \cdot m)/^\circ$ and k_ψ = 0.55 $(N \cdot m)/^\circ$. These gains were hand-tuned by the authors to obtain a fast response to human motions while maintaining system stability. Figure 3 shows results for a tracking experiment using this controller. We achieve good tracking on the θ-axis, and a small phase lag is visible on the ψ-axis.

D. Packet Design

As noted briefly in the introduction, our torque output controller operates through the use of position command packets. The angular momentum of the flywheel must be changed to produce an output torque. This is ideally performed by changing the orientation of the rotational axis of the flywheel, since it provides a mechanical advantage. However, the orientation of the output torque also changes with reorientation of the flywheel. This effect is described in (2). Thus, we developed a packet-based algorithm for controlling the gimbal axes. These packets are designed to maximize the magnitude of the desired torque for a short duration in the desired direction, while also minimizing the change in orientation during that impulse, and minimizing a rebound torque. The rebound torque is an undesired torque applied to the user when a gimbal is returning to its home configuration.

Several different packet designs were devised in order to produce a momentary output torque in a desired direction [6]. It is known from the dynamic model that if an acceleration is applied along one axis of a gimbal initially at rest, an output torque along an orthogonal axis will occur. As such, the design of the ideal packet will start with the naive application of an acceleration without concern for the ending configuration of the flywheel. An example of this naive approach is shown in Figure 4. The reader should note the continued torque output by the device when the velocity of the θ-axis is non-zero. By accelerating the θ-axis, a desirable output torque is produced. However, the gimbal must return to a non-moving state in order to cease production of the output torque.

The initial naive design may be extended into a doublet by providing a positive acceleration on the θ-axis, followed by a negative acceleration of the same magnitude and duration. This rapidly accelerates and decelerates the gimbal, resulting in zero velocity after the desired torque has been produced. Simulated results of such an experiment can be seen in Figure 5. However, this packet leaves the active gimbal in a configuration away from its home position. Remember that the workspace of output torques at any given instant is normal to the axis of rotation of the flywheel. For our purposes, we will assume that the next output torque to be generated is in a plane defined around the home position of the flywheel. One should be able to see how anticipation of a desired torque would dictate the configuration of the flywheel.

To return the gimbal to the home position, a second acceleration doublet with a longer duration, smaller magnitude, and starting with a negative instead of a positive acceleration should be applied. The integral of the positive component of both doublets should be equal, as should the integral of the negative components of each doublet. This ensures that the gimbal returns to the starting home position. Such a packet

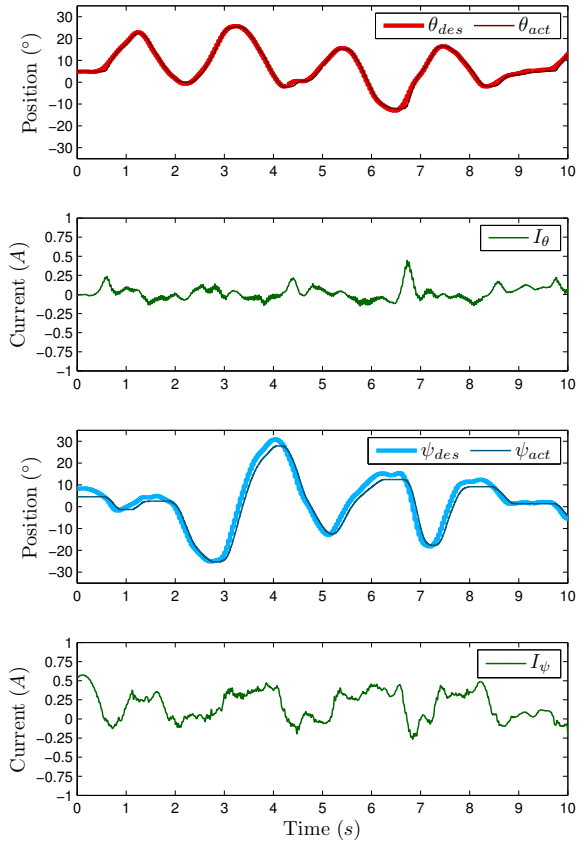

Fig. 3: Tracking response of the gimbal during gentle hand movements. Both degrees of freedom show good tracking, though the position errors are larger on the ψ-axis. We believe these larger errors and the corresponding abrupt changes in current output stem from the presence of significant static friction on this axis. One can also see a slight phase lag on the ψ-axis due to the digital control algorithm.

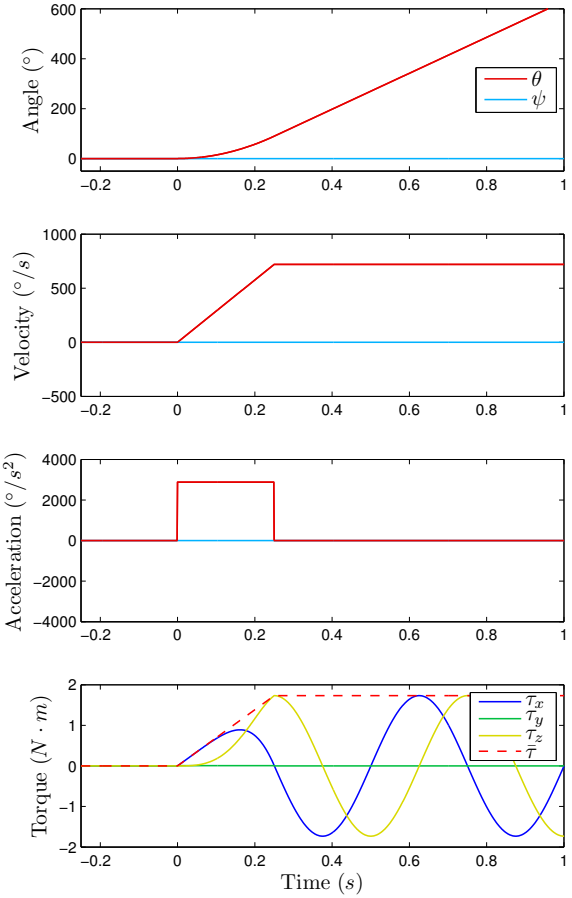

Fig. 4: The most naive packet design and its effect on the dynamic model. Torque output continues after the initial desired moment.

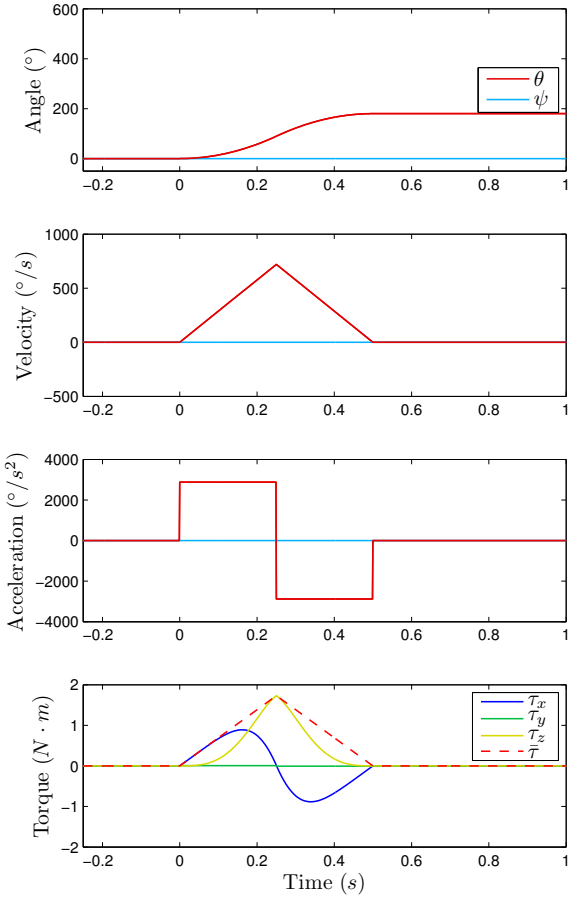

Fig. 5: An improved packet, consisting of an acceleration doublet, along with its effect on the dynamic model. The gimbal is brought to rest, but it is not returned to its home position.

will produce a fairly good match to our desired torques, but it can be refined ever further. On the rebound to the home position, it is desirable to minimize the torque ${}^{\theta}\vec{M}_{fw}$ while still making progress towards the home position. One should notice that the net torque will be smaller if we set one of the two components of (2) equal to zero. However, the velocity component (ω) cannot be set to zero without an acceleration component ($\dot{\omega}$). Instead, the acceleration can be set to zero at some point in time so that there is a constant velocity. Taking advantage of this, the packet can have an initial doublet followed by a small negative acceleration, then zero acceleration with a sustained non-zero velocity, finally followed by a small positive acceleration. As shown in Figure 6, this final packet design returns the gimbal to the home position and produces a relatively small undesired output torque.

V. Experimental Validation

In order to validate both the model and the packet design, a series of experiments with several packet types was performed. The results of the best packet discussed above are shown here.

A. Test Setup

For all tests, the inertial measurement unit was removed and replaced with an ATI Mini40 SI force/torque sensor, as shown in Figure 7. The other side of this sensor was then firmly attached to a desk so that the handle was in an upright position. This configuration was chosen to minimize the effects seen from gravity.

B. Packet Tests

Figure 8 shows one trial of the previously described packet along with simulated results. The model closely matches the measurements for the x-axis, which is the desired output axis. Note that the measured and predicted bias torques due to gravity have been removed in order to reduce errors due to sensor calibration.

VI. World Haptics 2009 Demonstration

The iTorquU 2.1 was demonstrated at the IEEE World Haptics Conference on March 19 and 20, 2009, in Salt Lake City, Utah, USA. This demonstration exhibited a falling virtual ball that users could catch on a virtual board. The board was then torqued by the transfer of energy from the ball to the board, and the user felt this torque via actuation

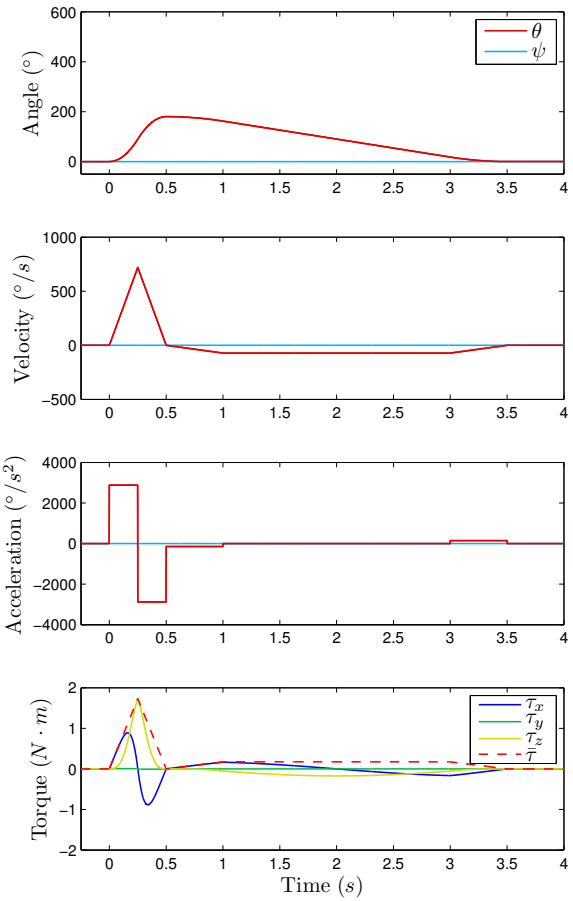

Fig. 6: Our chosen packet and its effect on the dynamic model. The packet begins with a large acceleration doublet to give the flywheel a high angular velocity. This is followed by a small negative acceleration to start the flywheel moving back toward the home position. Acceleration is then set to zero after some nominal time to keep a constant slow velocity. Once the gimbal is near its home position, a small positive acceleration is applied to leave it at the home position with zero velocity.

of the gimbal. Figure 9 shows one sample of the impulse delivered to a user's hand and the resulting perturbation in the person's configuration relative to ground.

Although the gyroscopic effect was first described in the early 19th century, it nonetheless continues to intrigue those who encounter it. The idea that a device is able to create torques without the use of a grounded object for leverage creates a sense of mystery. We found that the same was true during the demonstration at World Haptics. When the iTorqU exerted a torque on the user's hand, the user was almost always surprised by the effect, with several people commenting that the device felt alive. We noticed that this was the case even among those individuals who were familiar with the gyroscopic effect.

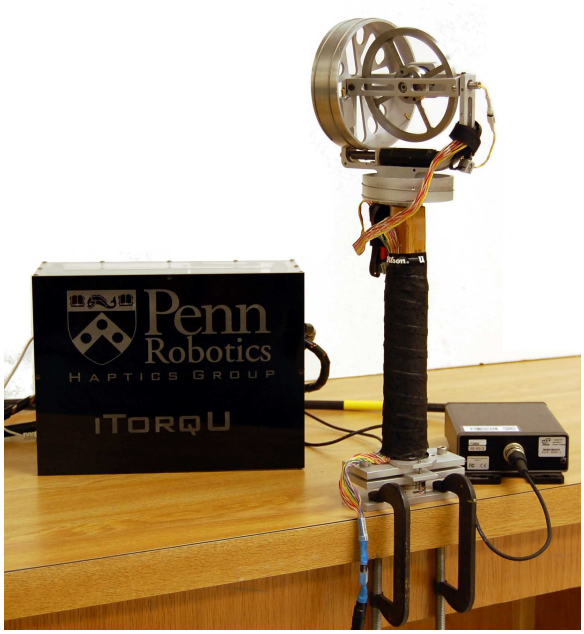

Fig. 7: The device configuration used for testing. An ATI Mini40 force/torque sensor is secured to the table with an adapter plate and c-clamps. The bottom of the iTorqU is then secured to the Mini40 with a series of plates. Also shown on the left is the linear amplifier control box, and on the right is the ATI amplifier box.

VII. Conclusion

This paper describes the design and control of a new ungrounded torque feedback device. A dynamic model of the iTorqU 2.1 was created, and two different control modes were developed for its operation. The first control mode is a transparency controller. This algorithm was designed to maintain a flywheel-to-ground configuration within the limits of human hand movement. The transparency controller proved successful through experimental validation. A second algorithm was developed to produce specific output torques using a *position-p-at-time-t* packet system. The model was used to guide development of an ideal packet. This packet was tested experimentally with a multi-axis torque sensor. Results from these tests aligned well with predictions from the model, though some discrepancies were noted, particularly in the z-axis torque. The device was demonstrated at the IEEE World Haptics Conference in 2009 and showed that it could generate torques that significantly perturb a user's hand. Users also commented on the novel and compelling feel of ungrounded torques.

Future studies should focus on combining this work with that of [9], so that torques can be generated from an arbitrary device configuration. This could allow for delivery of ungrounded torque feedback without necessarily returning the gimbals to a home position. Continued research should also focus on the generation of desired torques when the user is actively rotating the device. This would require sensing device perturbations and correcting the *position-p-at-time-t* packet for the instantaneous configuration.

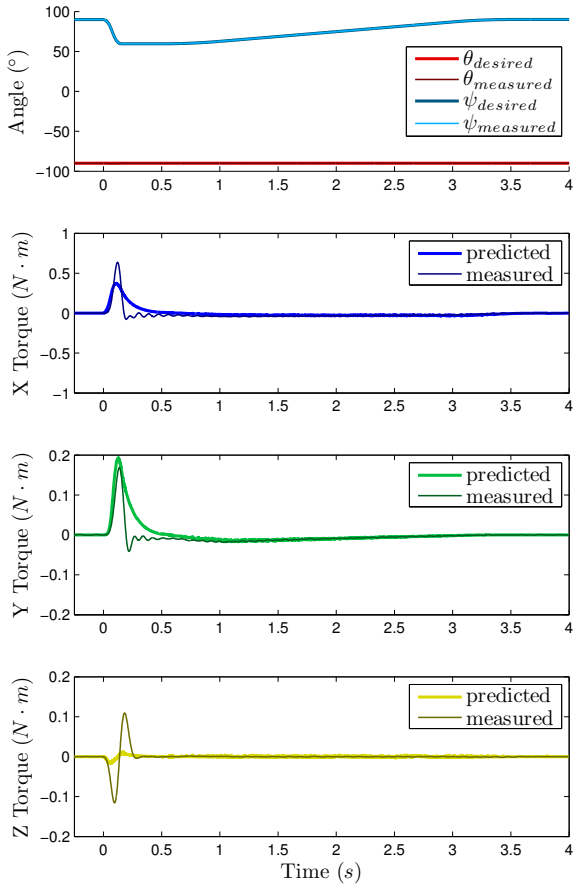

Fig. 8: Results of a test where the ψ-axis (the gimbal's lower axis) executed a packet of the final design; the iTorqU was attached to the test rig shown in Fig. 7, so its handle was not permitted to move. The moments generated around the x- and y-axes follow the model predictions quite well. The measured moment on the x-axis is slightly higher than expected, but it retains the anticipated shape. The moment measured around the z-axis is significantly larger than expected; we believe this discrepancy is due to imperfections in the hardware, such as non-orthogonal axes.

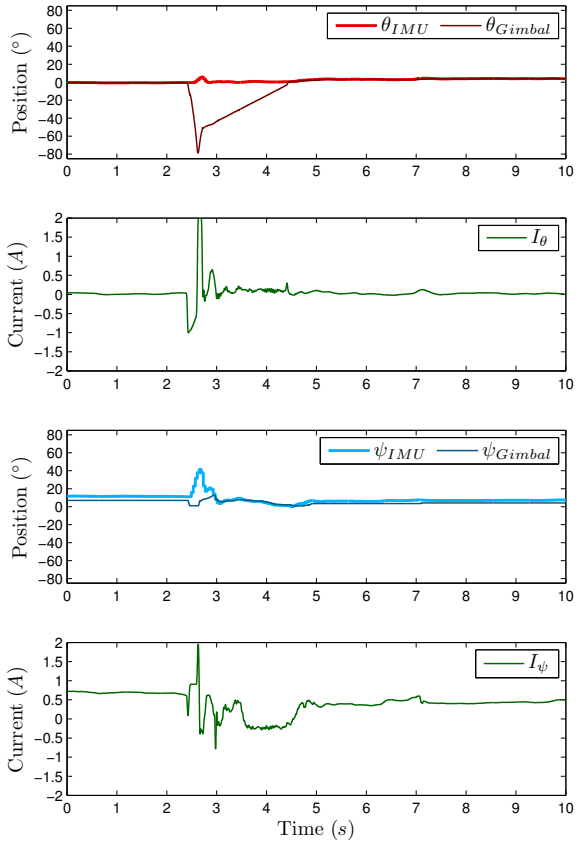

Fig. 9: Results of a test where the θ-axis (the gimbal's upper axis) executed a packet similar to our final design that was shown in Figure 8; the iTorqU was held in a user's hand, so its handle was permitted to move. The generated torque perturbed the user's hand by approximately 30° on the ψ-axis.

References

[1] V. Hayward and K. Maclean. Do it yourself haptics: part I. *IEEE Robotics & Automation Magazine*, 14(4):88–104, December 2007.

[2] T. H. Massie and J. K. Salisbury. The PHANToM haptic interface: a device for probing virtual objects. In *Proceedings of the ASME Winter Annual Meeting, Symposium on Haptic Interfaces for Virtual Environments and Teleoperator Systems*, Chicago, IL, 1994.

[3] J. B. Scarborough. *The Gyroscope: Theory and Applications*. Interscience Publishers Inc., 1 edition, 1958.

[4] C. Swindells, A. Unden, and T. Sang. TorqueBAR: an ungrounded haptic feedback device. In *Proceedings of the 5th International Conference on Multimodal Interfaces, Vancouver, British Columbia, Canada*, Nov. 2004.

[5] Y. Tanaka, J. Yamashita, and N. Nakamura. Mobile torque display and haptic characteristics of human palm. In *Proceedings of ICAT 2001, Tokyo, Japan*, pages 115–120, Dec. 2001.

[6] K. N. Winfree. An ungrounded haptic torque feedback device: The iTorqU. Master's thesis, University of Pennsylvania, Aug. 2009.

[7] K. N. Winfree, J. Gewirtz, T. Mather, J. Fiene, and K. J. Kuchenbecker. A high-fidelity ungrounded torque feedback device: The iTorqU 2.0. In *Proceedings of the 2009 World Haptics Conference*, pages 261–266, Mar. 2009. Hands-on demonstration presented at this conference.

[8] H. Yano, M. Yoshie, and H. Iwata. Development of a non-grounded haptic interface using the gyro effect. In *Proceedings of 11th International Symposium on Haptic Interfaces for Virtual Environment and Teleoperator Systems*, pages 32–39, 2003.

[9] M. Yoshie, H. Yano, and H. Iwata. Movement instruction using gyro effect generated with human motion (in Japanese). In *Proceedings of the Virtual Reality Society of Japan Annual Conference*, pages 273–276, 2002.